

## A facile strategy to prepare functionalized graphene *via* intercalation, grafting and self-exfoliation of graphite oxide

Lei Chen, Zhiwei Xu,\* Jialu Li, Yinglin Li, Mingjing Shan, Chunhong Wang, Zhen Wang, Qiwei Guo, Liangsen Liu, Guangwei Chen and Xiaoming Qian

Received 27th February 2012, Accepted 28th May 2012

DOI: 10.1039/c2jm31208e

**A facile method of successive intercalation, grafting and exfoliation of graphite oxide in monomers by  $\gamma$ -ray irradiation to obtain functionalized graphene nanosheets was reported. The monolayer percentage of functionalized graphene nanosheets was sharply increased and the agglomeration showed a significant decrease.**

Currently, facile and proper chemical functionalization of graphene nanosheets (GNS) has been proposed to prevent their irreversible aggregation, improve their solubility in organic solvents and facilitate synthesis of graphene-polymer composites. There have been a mass of remarkable achievements in the field of graphene-based functionalization.<sup>1–5</sup> However, in view of large scale applicability of functionalized graphene nanosheets, several issues arise, which include scalability, simplification, low-cost and stability. Recently, as an extremely versatile carbon system, the rediscovering of graphite oxide (GO) provides the possibility of producing functionalized graphene nanosheets efficiently owing to its easy intercalation and exfoliation properties. In addition, the functionalization of GO could also be facilitated by the tunable oxygen functional groups on the sheets.<sup>6,7</sup> Until now, the traditional method for preparing functionalized graphene nanosheets is the functionalization of the reduced graphene oxide, which was fabricated from chemical exfoliation and reduction of GO.<sup>8,9</sup> Nevertheless, reduction typically causes irreversible particle aggregation in solvents due to the prominent interlayer  $\pi$ - $\pi$  conjugate interaction of the graphene nanosheets.<sup>10,11</sup> This aggregation will significantly weaken the effect of functionalization and the treatment is time-consuming, high-cost, small-scale and complicated. Moreover, the traditional procedure with functionalization after exfoliation would also cripple the effect of functionalization. Hence, it is imperative to find a technique to realize a procedure for complete functionalization of GO before exfoliation. However, the interlayer functionalization of GO cannot be achieved by most of the existing covalent or non-covalent ways. Fortunately,  $\gamma$ -rays have been extensively investigated as a scalable, simple and cost-effective technique to control the properties of carbon systems.<sup>12–14</sup> More impressively, the

strong penetration power of  $\gamma$ -rays makes them a promising candidate for the complete and especially interlayer functionalization of GO.

To verify the feasibility of the strategy, here we reported a method to prepare functionalized graphene nanosheets by a  $\gamma$ -ray irradiation of GO in styrene. The potential procedures with the orders of intercalation, grafting and then exfoliation are expected to prevent the agglomeration of functionalized graphene nanosheets. The GO and irradiated GO (IGO) were characterized by means of Fourier transform infrared (FT-IR) spectra, X-ray photoelectron spectroscopy (XPS), Raman spectra, X-ray diffraction (XRD), atomic force microscopy (AFM), transmission electron microscope (TEM), high resolution TEM (HR-TEM) and thermogravimetric analysis (TGA). The  $\gamma$ -ray irradiation strategy was proved to present an efficient way to enhance the domination of the scalable functionalization of graphene nanosheets with high percent of monolayers and little agglomeration in one step.

GO was prepared according to the method in ref. 8. Typically, GO (100 mg) and styrene-toluene (50 mL : 50 mL) were mixed and sonicated for 5 min to disperse the solids homogeneously. The mixture was then exposed to <sup>60</sup>Co  $\gamma$ -ray source in an absorbed dose 200 kGy with 2.0 kGy h<sup>-1</sup> dose rate at room temperature. After irradiation, the GO-styrene mixture was purified repeatedly by cycling-membrane filtration/tetrahydrofuran (THF)-redispersion until no white emulsion precipitated when the filtrate was added to water. The precipitate was then dried in a vacuum oven at 50 °C for 24 h to get IGO (106.7 mg). In addition, functionalized graphene nanosheets were prepared by dissolving IGO in THF. For comparison, pristine GO was sonicated in the deionized water for 2 h to get the graphene oxide nanosheets. The chemical character and morphology of pristine GO and IGO were analyzed by XRD (1.54059 Å Cu K $\alpha$  1 as wavelength), Raman (RENISHAW inVia Raman Microscope, recorded using 514 nm laser excitation with a power of 5 mW), XPS (Thermo ESCALAB 250) and FT-IR spectra (Bruker VECTOR-22 IR spectrometer), respectively. AFM (CSPM5500), TEM (Tecnai G2 F20) and HR-TEM (Tecnai G2 F20) observations were conducted for graphene oxide nanosheets and functionalized graphene nanosheets. The samples for AFM analyses were precisely prepared by depositing these two kinds of nanosheets on cleaved mica surfaces respectively. The degree of grafting was estimated by TGA (NETZSCH STA 409 PC/PG) and was calculated using eqn (1):<sup>15</sup>

Key Laboratory of Advanced Braided Composites, Ministry of Education, School of Textiles, Tianjin Polytechnic University, Tianjin 300160, People's Republic of China. E-mail: xuzhiwei@tjpu.edu.cn; Fax: +86 022 83955231; Tel: +86 022 83955231

$$DG(\%) = \frac{R_G - R}{R_G - R_P} \times 100\% \quad (1)$$

wherein,  $R_G$ ,  $R$  and  $R_P$  represent the residual weight percentage (wt%) of GO, IGO and polystyrene (PS) pyrolysis, respectively. For comparison, structures of GO irradiated in toluene under the same conditions were also investigated.

We applied X-ray techniques to determine the changes in the interlayer spacing of GO, which maybe interpreted as a partial or complete introduction into the interlayer spacing by some molecular species. XRD patterns for the GO, sonicated GO and IGO are recorded in Fig. 1(a). We can see that the peak corresponding to the 0.95 nm interlayer spacing appears to be retained after slight ultrasonic processing.<sup>8</sup> However, the van der Waals forces seem to be insufficient to maintain GO stacking due to the intercalation and grafting of PS induced by the high energy  $\gamma$ -rays. The (002) peak has almost disappeared in IGO, presumably because of introduction of PS functional groups between the GO layers, grafting of PS chains on the sheets and then exfoliation of GO induced by the  $\gamma$ -ray irradiation.

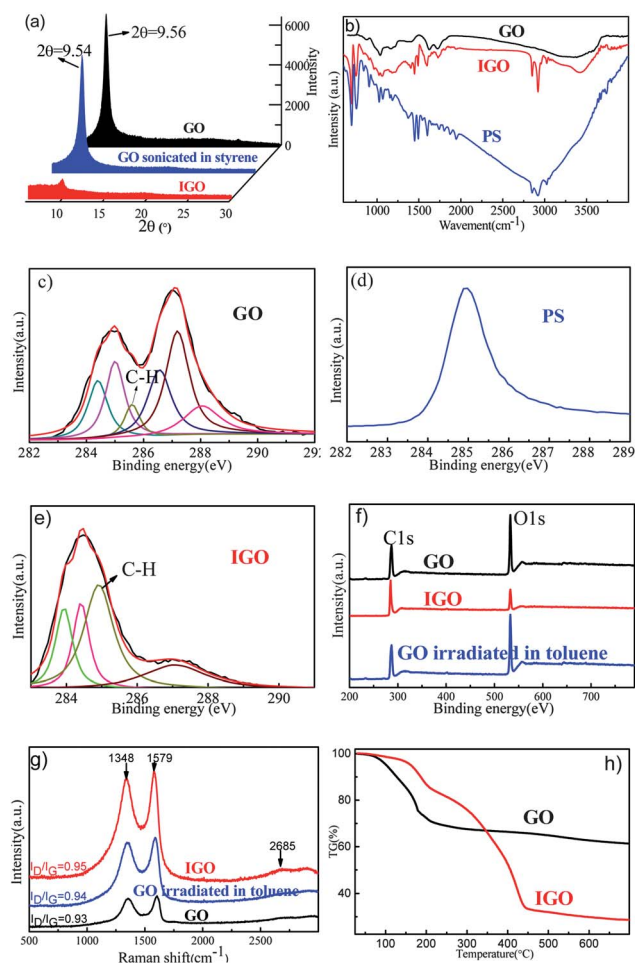


**Fig. 1** (a) XRD patterns of GO, GO sonicated in styrene and IGO, (b) FT-IR spectra of GO, PS and IGO, (c) C1s spectra of GO, (d) C1s spectra of PS, (e) C1 spectra of IGO, (f) XPS full-scan spectra of GO, IGO and GO irradiated in toluene, (g) Raman spectra of GO, GO irradiated in toluene and IGO and (h) TG curves (in  $N_2$ ) of GO and IGO with a heating rate of  $5^\circ C\ min^{-1}$ .

To verify that we have achieved one-step intercalation and functionalization of GO by  $\gamma$ -rays in styrene, we carried out the FT-IR mapping of GO, PS and IGO (Fig. 1(b)). The FT-IR spectrum of IGO exhibits characteristic vibrations bands for PS (absorbance peaks at 3026, 1597, 1491, 750, and  $696\ cm^{-1}$  correspond to the phenyl group, the peaks at 2920 and  $2850\ cm^{-1}$  represent the emergence of methylene and methenyl groups, and the peaks at 1448 and  $1404\ cm^{-1}$  could be assigned to saturated and unsaturated C–H bonds).<sup>2,16</sup> This is in accordance with the XRD data of the samples and accounts for the good introduction of PS functional group which is induced by  $\gamma$ -irradiation effect in styrene. This bonding of the PS chains should be covalent due to the fact that IGO was washed repeatedly with the powerful solvent THF to remove the physically absorbed PS away. In addition, the phenomenon that a significant alternation in the relative intensity of  $-OH$  ( $\sim 3420\ cm^{-1}$ ),  $-C=O$  ( $\sim 1058\ cm^{-1}$ ) and  $-COOH$  ( $\sim 1726\ cm^{-1}$ ) cannot be found in the FT-IR spectrum could be explained by the grafting of PS functional groups mostly on the GO basal plane. The presence of PS in GO composites can be further confirmed by XPS (Fig. 1(c–f)), which provides rich information about the functional groups intercalating into the layers of GO. Curve fitting of the GO and IGO C1s spectra are performed using a Gaussian–Lorentzian peak shape after performing a linear background correction and the results are shown in Fig. 1(c) and (e). The binding energy of C–C and C–H bonding are assigned at 284.8–285.3 eV.<sup>17–20</sup> The grafting of PS chains is supported by the intensity increase in C–H absorption peak ( $\sim 285.2\ eV$ , Fig. 1(d)) in IGO C1s core shell spectrum.<sup>17</sup> This bonding effect is verified again from the XPS survey of GO, IGO and GO irradiated in toluene in Fig. 1(f).<sup>16</sup> All spectra reveal the presence of mainly carbon (284.6 eV) and oxygen (532.3 eV). For pristine GO, the relative atomic concentrations of carbon and oxygen are 64.12 and 34.93%, respectively. These two values are slightly changed to 63.12 and 33.93% after irradiation in toluene. However, when irradiated in styrene, the atomic concentrations of carbon and oxygen in the IGO are altered to 78.93 and 20.88%, further confirming the bonding of the PS-chains on the plane.

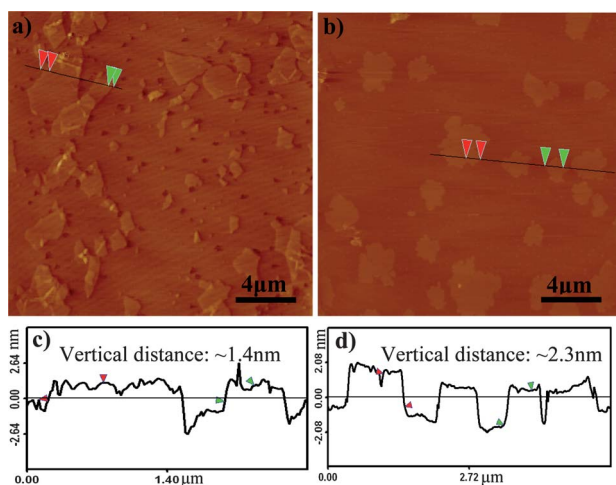
It is worth noting that the percentage of the oxygen in IGO is dramatically decreased (Fig. 1(d)) owing to the significant increase of C–H which is induced by the covalent attachment of the PS chains. However, the XRD peak of IGO doesn't shift to the characteristic adsorbing band of graphene ( $\sim 24^\circ$ )<sup>21</sup> due to the fact that there is little reduction effect on GO induced by  $\gamma$ -rays. In addition, the survey spectrum of IGO (Fig. 1(f)) shows quite some amount of oxygen, which strongly supports that the final products actually being PS-grafted graphene nanosheets with a high percentage of monolayers which still have a number of oxygen groups.

The bands at 1348 and  $1579\ cm^{-1}$  in the Raman spectra (Fig. 1(g)) are assigned to the G band (associated with the vibration of  $sp^2$  carbon atoms in a graphitic 2D hexagonal lattice) and D band (related to the vibrations of  $sp^3$  carbon atoms of defects and disorder).<sup>22</sup> The intensity ratio of D band to G band ( $I_D/I_G$ ) of GO are shown to be increased from 0.93 to 0.95 after irradiation in styrene, suggesting a decrease in the average size of  $sp^2$  carbon domains, which is induced by the increased number of smaller graphitic domains formed during the irradiation process.<sup>23,24</sup> Moreover, this weak increase may also suggest the covalently bonding of PS chains on graphene nanosheets and support the cutting effects (from the AFM results) under irradiation.<sup>16,25</sup> The intensity of the overtone 2D-band with respect to the D- and G-band is small.

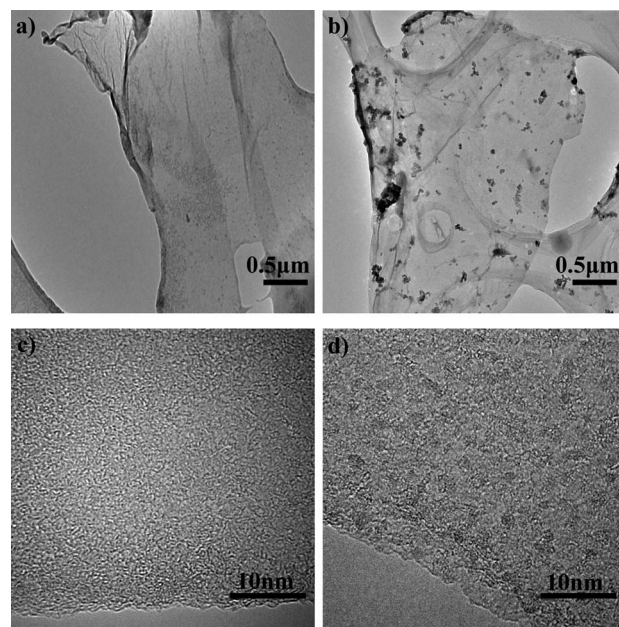
The 2D peak at  $\sim 2700\text{ cm}^{-1}$  is obviously increased after the  $\gamma$ -ray treatment in styrene, strongly suggesting the reality of using edge and basal plane defects to allow an analogous photo-polymerization process without disturbing the conjugation of the as-prepared material. Furthermore, the change of  $I_D/I_G$  before and after irradiation is very limited, implying the functionalization is completed and aromaticity of the IGO should be partially restored due to the annealing effect.<sup>24,26,27</sup> In addition, there is also no obvious alteration of the  $I_D/I_G$  when irradiating GO in toluene (Fig. 1(g)).

Fig. 1(h) shows the TGA curves of GO and IGO in the temperature range from 25 to 700 °C. There are two clearly separated weight loss stages in the range of 120–220 °C and 320–460 °C for IGO, which corresponding to GO (ref. 15) and grafted PS.<sup>16</sup> The residual weights of GO and IGO after 700 °C were 28.67 wt% and 61.35 wt%, respectively. Assuming that the grafted PS chains were completely pyrolyzed, the weight percent of grafted PS chains was as high as 53.27 wt%, as calculated according to eqn (1).

The AFM images (Fig. 2) of GO and IGO indicate the results of less aggregation and more monolayers of graphene nanosheets brought by this strategy. Due to the extensive oxidation in the preparation procedure, the thicknesses of pristine GO single-layer sheets we prepared are mostly within a range of 1.2–1.5 nm (Fig. 2(a) and (c)), which is a little higher than that reported.<sup>28–30</sup> In addition, some graphene sheets are shown as multi-layers from Fig. 2(a) because of the overlapping or aggregation in pristine samples. Fig. 2(b) and Fig. 2(d) show that the heights of IGO sheets are about 1.9 nm to 2.4 nm. It is noteworthy that the height value may be higher than that of the pristine GO monolayers but lower than bilayers due to the PS chains grafted on the nanosheet surfaces or trapped underneath the drop-dried SP-graphene flake ‘coffee rings’.<sup>31</sup> The results can also be observed by TEM and HR-TEM. Fig. 3(a) and (c) depict the transparent flake-like shape of GO sheets on the micro-grid film. After irradiation, some dark features can be observed on the IGO sheets as shown in Fig. 3(b) and (d). This may due to the pisolitic aggregates formed on surface of GO sheet by encircling with PS chains. Since this polymerization happens on the nanosheets, it is



**Fig. 2** Tapping mode AFM topographic images of (a) graphene nanosheets from the GO sonicated for 2 h, (b) graphene nanosheets from the dispersed IGO in THF, (c) cross-section of graphene nanosheets from the sonicated GO and (d) cross-section of graphene nanosheets from the dispersed IGO in THF.



**Fig. 3** TEM images for (a) GO and (b) IGO and HR-TEM images for (c) GO and (d) IGO.

reasonable to find the aggregation of nanosheets linked by the polystyrene chains. However, the AFM and XRD results showed that the incidence of this linkage or aggregation should be very low. Thus, instead of overlapping (Fig. 2(a) and (b)), IGO sheets show mainly separating from each other so that graphene nanosheets with high percentage of monolayers are well established. It can also be found from Fig. 2(b) that some vacancies are formed after irradiation, making the boundaries and the surface of the sheets a little more ‘bumpy’ than the pristine ones due to the cutting effect of  $\gamma$ -rays.<sup>32,33</sup>

The schematic comparison of our strategy and the traditional method to prepare functionalized graphene nanosheets is given in Fig. 4. Obviously, due to the extensive exfoliation (from the XRD results), the functionalized graphene nanosheets with a high percentage of single-layer graphene are evidenced to be prepared by  $\gamma$ -ray irradiation. In addition, our strategy is also a way for the preparation of functionalized graphene nanosheets with much less

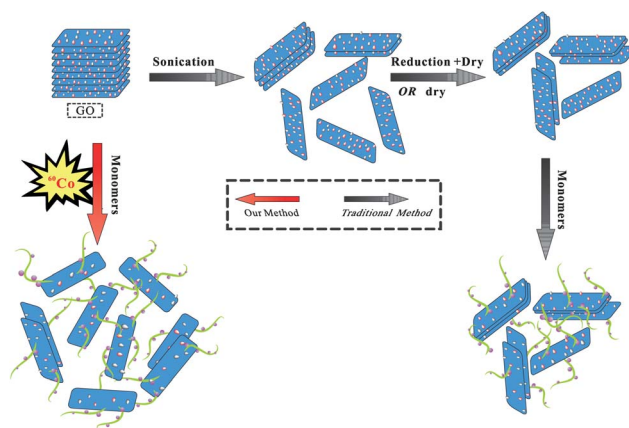


**Fig. 4** Schematic drawing of a comparison of the functionalization of graphene nanosheets by our strategy and the traditional method.



agglomeration than the traditional method. It should be attributed to the fact that interlayer functionalization of GO in our experiment is designed to be achieved *via* high energy  $\gamma$ -rays before exfoliation. The aggregation and the restacking through van der Waals interactions are reduced significantly owing to the bonding of long PS chains on the planes.<sup>34</sup> Moreover, the elimination of the drying procedure also plays a significant role in preventing agglomeration.

In conclusion, based on the design idea of GO interlayer functionalization before exfoliation, we have prepared functionalized graphene nanosheets with the potential order of intercalation, grafting and exfoliation of GO by a one-step  $\gamma$ -ray irradiation protocol. This strategy is proved to provide a route to truly produce functionalized graphene nanosheets with little agglomeration and a high percentage of monolayers under the combined action of our distinctive design concept and  $\gamma$ -ray technique with high penetration power. Due to the cutting effect induced by  $\gamma$ -ray irradiation, some vacancies are formed in the functionalized graphene nanosheets, making the boundaries and the surface of the sheets a little more 'bumpy' than the pristine ones. The cutting phenomenon can also be supported by the increased value of  $I_D/I_G$ . Given the low-cost, large-scale and high-efficient of the preparing strategy, and high percent of monolayers and little agglomeration of products, the one-step  $\gamma$ -ray irradiation of GO in monomers is expected to be used as a promising industrial route for the bulk preparation of functionalized graphene nanosheets.

## Notes and references

- 1 S. Stankovich, D. A. Dikin, G. H. B. Dommett, K. M. Kohlhaas, E. J. Zimney, E. A. Stach, R. D. Piner, S. T. Nguyen and R. S. Ruoff, *Nature*, 2006, **442**, 282.
- 2 M. Steenackers, A. M. Gigler, N. Zhang, F. Deubel, M. Seifert, L. H. Hess, C. H. Y. X. Lim, K. P. Loh, J. A. Garrido, R. Jordan, M. Stutzmann and I. D. Sharp, *J. Am. Chem. Soc.*, 2011, **133**, 10490.
- 3 E. D. Grayfer, A. S. Nazarov, V. G. Makotchenko, S. J. Kim and V. E. Fedorov, *J. Mater. Chem.*, 2011, **21**, 3410.
- 4 Y. Si and E. T. Samulski, *Nano Lett.*, 2008, **8**, 1679.
- 5 R. Hao, W. Qian, L. H. Zhang and Y. L. Hou, *Chem. Commun.*, 2008, 6576.
- 6 T. Szabo, E. Tombacz, E. Illes and I. Dekany, *Carbon*, 2006, **44**, 537.
- 7 M. Hirata, T. Gotou, S. Horiuchi, M. Fujiwara and M. Ohba, *Carbon*, 2004, **42**, 2929.
- 8 D. C. Marcano, D. V. Kosynkin, J. M. Berlin, A. Sinitskii, Z. Z. Sun, A. Slesarev, L. B. Alemany, W. Lu and J. M. Tour, *ACS Nano*, 2010, **4**, 4806.
- 9 S. Stankovich, D. A. Dikin, R. D. Piner, K. A. Kohlhaas, A. Kleinhammes, Y. Jia, Y. Wu, S. T. Nguyen and R. S. Ruoff, *Carbon*, 2007, **45**, 1558.
- 10 L. J. Cote, F. Kim and J. X. Huang, *J. Am. Chem. Soc.*, 2009, **131**, 1043.
- 11 M. Lotya, Y. Hernandez, P. J. King, R. J. Smith, V. Nicolosi, L. S. Karlsson, F. M. Blighe, S. De, Z. M. Wang, I. T. McGovern, G. S. Duesberg and J. N. Coleman, *J. Am. Chem. Soc.*, 2009, **131**, 3611.
- 12 Z. Xu, L. Chen, L. Liu, X. Wu and L. Chen, *Carbon*, 2011, **49**, 350.
- 13 Z. W. Xu, Y. D. Huang, C. H. Zhang, L. Liu, Y. H. Zhang and L. Wang, *Compos. Sci. Technol.*, 2007, **67**, 3261.
- 14 S. A. Vitusevich, V. A. Sydoruk, M. V. Petrychuk, B. A. Danilchenko, N. Klein, A. Offenhausser, A. Ural and G. Bosman, *J. Appl. Phys.*, 2010, **107**, 063701.
- 15 B. W. Zhang, Y. J. Zhang, C. Peng, M. Yu, L. F. Li, B. Deng, P. F. Hu, C. H. Fan, J. Li and Q. Huang, *Nanoscale*, 2012, **4**, 1742.
- 16 H. X. Xu, X. B. Wang, Y. F. Zhang and S. Y. Liu, *Chem. Mater.*, 2006, **18**, 2929.
- 17 Y. L. Liu and W. H. Chen, *Macromolecules*, 2007, **40**, 8881.
- 18 T. C. Chiang and F. Seitz, *Ann. Phys.*, 2001, **10**, 61.
- 19 S. Yumitori, *J. Mater. Sci.*, 2000, **35**, 139.
- 20 D. Yang, A. Velamakanni, G. Bozoklu, S. Park, M. Stoller, R. D. Piner, S. Stankovich, I. Jung, D. A. Field, C. A. Ventrice and R. S. Ruoff, *Carbon*, 2009, **47**, 145.
- 21 H. J. Shin, K. K. Kim, A. Benayad, S. M. Yoon, H. K. Park, I. S. Jung, M. H. Jin, H. K. Jeong, J. M. Kim, J. Y. Choi and Y. H. Lee, *Adv. Funct. Mater.*, 2009, **19**, 1987.
- 22 M. Dehonor, K. Varlot-Masenelli, A. Gonzalez-Montiel, C. Gauthier, J. Y. Cavaille, H. Terrones and M. Terrones, *Chem. Commun.*, 2005, 5349.
- 23 M. S. Dresselhaus, A. Jorio, M. Hofmann, G. Dresselhaus and R. Saito, *Nano Lett.*, 2010, **10**, 751.
- 24 S. Dannefaer, A. Pu, V. Avalos and D. Kerr, *Physica B*, 2001, **308–310**, 569.
- 25 Y. Lin, B. Zhou, K. A. S. Fernando, P. Liu, L. F. Allard and Y. P. Sun, *Macromolecules*, 2003, **36**, 7199.
- 26 M. S. Dresselhaus, A. Jorio, M. Hofmann, G. Dresselhaus and R. Saito, *Nano Lett.*, 2010, **10**, 751.
- 27 M. Fang, K. G. Wang, H. Lu, Y. L. Yang and S. Nutt, *J. Mater. Chem.*, 2010, **20**, 1982.
- 28 Z. H. Ni, H. M. Wang, J. Kasim, H. M. Fan, T. Yu, Y. H. Wu, Y. P. Feng and Z. X. Shen, *Nano Lett.*, 2007, **7**, 2758.
- 29 J. Inhwa, M. Vaupel, M. Pelton, R. Piner, D. A. Dikin, S. Stankovich, A. Jinho and R. S. Ruoff, *J. Phys. Chem. C*, 2008, **112**, 8499.
- 30 C. Chen, Q.-H. Yang, Y. Yang, W. Lv, Y. Wen, P.-X. Hou, M. Wang and H.-M. Cheng, *Adv. Mater.*, 2009, **21**, 3541.
- 31 Z. Jin, T. P. McNicholas, C. J. Shih, Q. H. Wang, G. L. C. Paulus, A. Hilmer, S. Shimizu and M. S. Strano, *Chem. Mater.*, 2011, **23**, 3362.
- 32 J. Y. Li and Y. F. Zhang, *Appl. Surf. Sci.*, 2006, **252**, 2944.
- 33 J. Peng, X. X. Qu, G. S. Wei, J. Q. Li and J. L. Qiao, *Carbon*, 2004, **42**, 2741.
- 34 K. Jo, T. Lee, H. J. Choi, J. H. Park, D. J. Lee, D. W. Lee and B. S. Kim, *Langmuir*, 2011, **27**, 2014.